2816 *Inorg. Chem.* **2010**, *49*, 2816–2821
DOI: 10.1021/ic902196t

Inorganic Chemistry
Article

Molecular Geometry of Vanadium Dichloride and Vanadium Trichloride: A Gas-Phase Electron Diffraction and Computational Study

Zoltán Varga,[†] Brian Vest,[‡] Peter Schwerdtfeger,[‡] and Magdolna Hargittai*[,†]

[†]*Materials Structure and Modeling Research Group of the Hungarian Academy of Sciences, Budapest University of Technology and Economics, P.O. Box 91, 1521 Budapest, Hungary, and* [‡]*Centre for Theoretical Chemistry and Physics, New Zealand Institute for Advanced Study, Massey University* (*Auckland Campus*), *Private Bag 102904, North Shore MSC, 0745 Auckland, New Zealand*

Received November 6, 2009

The molecular geometries of VCl_2 and VCl_3 have been determined by computations and gas-phase electron diffraction (ED). The ED study is a reinvestigation of the previously published analysis for VCl_2. The structure of the vanadium dichloride dimer has also been calculated. According to our joint ED and computational study, the evaporation of a solid sample of VCl_2 resulted in about 66% vanadium trichloride and 34% vanadium dichloride in the vapor. Vanadium dichloride is unambiguously linear in its $^4\Sigma_g^+$ ground electronic state. For VCl_3, all computations yielded a Jahn−Teller-distorted ground-state structure of C_{2v} symmetry. However, it lies merely less than 3 kJ/mol lower than the $^3E''$ state (D_{3h} symmetry). Due to the dynamic nature of the Jahn−Teller effect in this case, rigorous distinction cannot be made between the planar models of either D_{3h} symmetry or C_{2v} symmetry for the equilibrium structure of VCl_3. Furthermore, the presence of several low-lying excited electronic states of VCl_3 is expected in the high-temperature vapor. To our knowledge, this is the first experimental and computational study of the VCl_3 molecule.

Introduction

The elusive structures of first-row transition metal dihalides continue to engage both experimentalists and theoreticians. Although it used to be a general belief that these molecules are all linear, spectroscopic studies for the early transition metal difluorides[1] and electron diffraction reports on VCl_2 and $CrCl_2$[2] suggested bent structures. On the other hand, spectroscopic studies of the dichlorides suggested linear structures.[3,4] When computations became feasible for transition metals, most of them suggested linear geometries but at the same time revealed that, especially for the early transition metal dihalides, rather close-lying electronic states can be expected.[5,6] Later computations found that for chromium dihalides the electronic ground-state structure is bent due to the Renner−Teller effect.[7−9] This structure was confirmed for both CrF_2 and $CrCl_2$ by combined electron diffraction and computational studies.[10,11] A recent vibrational spectroscopic study, on the other hand, found a linear structure for TiF_2 and suggested that no deviation from linearity can be expected for either of the first-row transition metal dihalides.[12]

The bent structure of $CrCl_2$ from its earlier ED study was the result of assuming a simpler vapor composition than was actually the case; the presence of trimers in the high-temperature vapor was ignored.[2] In the light of current information about these structures, a highly bent geometry of VCl_2 is unlikely. Hence, we decided on a reinvestigation of our ED data and augmented it with high-level computations. Although an early mass spectrometric study suggested that VCl_2 can be evaporated without decomposition,[13] later mass spectrometric studies indicated that both vanadium dichloride and vanadium trichloride are unstable at high temperatures.[14,15] Therefore, we had to assume that, besides the

*To whom correspondence should be addressed. E-mail: hargittaim@mail.bme.hu.

(1) Hastie, J. W.; Hauge, R. H.; Margrave, J. L. *J. Chem. Soc. Chem. Commun.* **1969**, 1452–1453.
(2) Hargittai, M.; Dorofeeva, O. V.; Tremmel, J. *Inorg. Chem.* **1985**, *24*, 3963–3965.
(3) Hastie, J. W.; Hauge, R. H.; Margrave, J. L. *High Temp. Sci.* **1971**, *3*, 257–274.
(4) Beattie, I. R.; Jones, P. J.; Willson, A. D.; Young, N. A. *High Temp. Sci.* **1990**, *29*, 53–62.
(5) Hargittai, M. *Chem. Rev.* **2000**, *100*, 2233–2301.
(6) Wang, S. G.; Schwarz, W. H. E. *J. Chem. Phys.* **1998**, *109*, 7252–7262.
(7) Bridgeman, A. J.; Bridgeman, C. H. *Chem. Phys. Lett.* **1997**, *272*, 173–177.
(8) Jensen, V. R. *Mol. Phys.* **1997**, *91*, 131–137.
(9) Nielsen, I. M. B.; Allendorf, M. A. *J. Phys. Chem. A* **2005**, *109*, 928–933.
(10) Vest, B.; Schwerdtfeger, P.; Kolonits, M.; Hargittai, M. *Chem. Phys. Lett.* **2009**, *468*, 143–147.
(11) Vest, B.; Varga, Z.; Hargittai, M.; Hermann, A.; Schwerdtfeger, P. *Chem.—Eur. J.* **2008**, *14*, 5130–5143.
(12) Wilson, A. V.; Roberts, A. J.; Young, N. A. *Angew. Chem., Int. Ed.* **2008**, *47*, 1774–1776.
(13) McCarley, R. E.; Roddy, J. W. *Inorg. Chem.* **1964**, *3*, 60–63.
(14) Ratkovskii, I. A.; Novikova, L. N.; Krisko, L. Y.; Rokashevich, E. M. *Russ. J. Phys. Chem.* **1976**, *50*, 302.
(15) Hildenbrand, D. L.; Lau, K. H.; Perez-Mariano, J.; Sanjurjo, A. *J. Phys. Chem. A* **2008**, *112*, 9978–9982.

 Published on Web 02/19/2010

evaporated dichloride, there might be other species as well in the vapor, possibly with vanadium in other oxidation states. Considering the high experimental temperature, certain species, such as VCl_4, cannot be expected to be present in the vapor. Vanadium dichloride, vanadium trichloride, and the dimer of vanadium dichloride are all possible candidates though; therefore, they all were subjected to computations.

Computational and Experimental Details

Computational Methodology. Due to the partial 3d-orbital occupation of vanadium in both the dichloride and the trichloride, all possible low-lying electronic states of VCl_2, VCl_3, and V_2Cl_4 were investigated. For VCl_2, the following electronic states were found close in energy (some of these states are strictly multireference in character): $^4\Sigma_g^+$ ($\delta_g^2\sigma_g^1$), $^4\Pi_g$ ($\delta_g^2\pi_g^1$), $^4\Delta_g$ ($\pi_g^2\delta_g^1$), and $^4\Phi_g$ ($\delta_g^1\pi_g^1\sigma_g^1$). Single-reference coupled-cluster including all single double and substitutions and noniterative triples as well as multireference calculations (CASPT2) were applied to determine the correct order of the different electronic states. For all state-specific CASPT2 calculations,[16] we chose the vanadium (3d4s4p) orbitals as the active CAS space; that is, for VCl_2 we distributed 3 electrons and for VCl_3 2 electrons in 9 orbitals. In these calculations, the 3s3p3d4s electrons of vanadium and all 17 electrons of each chlorine atom were correlated (47 electrons for VCl_2). Furthermore, different DFT methods were tested, and the unrestricted Kohn−Sham B3PW91[17,18] method was finally chosen for all further calculations, as the results were very close to our higher-level unrestricted CCSD(T) calculations,[19,20] where we used the full active orbital space within our pseudopotential approximation (see below); i.e., 13 electrons of vanadium and all 17 electrons of each chlorine were correlated. This, of course, introduces large spin-contamination especially in the DFT case but nevertheless can lead to accurate structures and energetics, as shown before for CrF_2 and $CrCl_2$.[10,11] The MP2 method,[21] as usual, underestimates the bond lengths. For the VCl_2 dimer, we only considered the ferromagnetically coupled (high-spin) septet and the antiferromagnetically coupled (low-spin) singlet electronic states, as an accurate treatment of all possible spin states is a formidable task. We only mention here that the triplet and quintet states are close in energy to the septet states. All single-reference computations were performed using the Gaussian03 program package.[22] For the multireference computations, the MOLPRO program was used.[23]

The vanadium atom was described by a relativistic small-core effective core potential (MDF ECP, describing 10 electrons)[24] and a corresponding valence basis set with a (13s12p11d4f3g)/[8s8p7d4f3g] contraction (aug-cc-pwCVTZ-PP).[25] For chlorine, a Dunning type all-electron cc-pVTZ basis set was used.[26]

To aid the ED analysis, the bending potential of the VCl_2 structures as well as the potential energy of the out-of-plane motion of the VCl_3 structures were calculated at the B3PW91 level of theory. For the two lowest-energy electronic states of VCl_2, the calculated bond-angle range was between 180° and 90° at 5° intervals. For the ground state of VCl_3, we need to consider the D_{3h}-symmetry $^3E''$ state undergoing Jahn−Teller distortion into C_{2v} symmetry, which either results in a $^3A_2$ or a $^3B_1$ state. The other possible electronic state is a $^3A_2'$ state of D_{3h} symmetry. In calculating the puckering potential for the different electronic states of VCl_3, the puckering was desribed by the perpendicular displacement of the central metal atom from the plane of the three chlorine atoms from 0 up to 1.00 Å, corresponding to bond angle changes from 120° to about 100° with increments of first 1° and later 2°. The contributions of the average structures were calculated from the computed energies of these structures by Boltzmann distribution for the experimental temperature.

The stability of all structures (if computationally possible) was verified by frequency calculations. Natural bond orbital (NBO)[27] and Wiberg bond index[28] analyses have also been carried out for all molecules.

Electron Diffraction Structure Analysis. The details of the electron diffraction experiment have been described previously.[2] The total diffraction intensities were taken from there, but a new background was drawn in the present analysis. The new experimental molecular intensities are given in the Supporting Information (Table S1). The experimental temperature was 1330(50) K.

All species corresponding to the possible products of evaporation and decomposition have been considered. A variety of vapor compositions were checked: VCl_2 and VCl_3 (**A**); VCl_2, VCl_3, and the dimer of VCl_2 (**B**), and, finally, the possibility that for both monomers all the close-lying electronic state molecules might also be present in the vapor (**C**). The following refinement scheme was used: The V−Cl bond length of VCl_3 was an independent parameter, and for the bond lengths of the other species, their differences from the above were taken from the DFT computations and constrained in the refinements. In addition, in refinement **B**, the bond angles of the dimer were also constrained at the computed values. In refinement **C**, in which all possible electronic state molecules were considered to be present, their contribution was calculated by a Boltzmann distribution based on the computed energy differences of these species.

The r_e computed bond length differences were converted to the operational r_a parameter by applying anharmonic corrections according to the expression $r_a \approx r_e + 3/2(al_T^2) - l_T^2/r$, where a is the Morse constant and l_T is the vibrational amplitude at the experimental temperature.[29] The starting value of the Morse constant was computed for the VCl diatomic molecule, but at later stages of the refinement it was determined from the

(16) Celani, P.; Werner, H. J. *J. Chem. Phys.* **2000**, *112*, 5546–5557.
(17) Perdew, J. P.; Chevary, J. A.; Vosko, S. H.; Jackson, K. A.; Pederson, M. R.; Singh, D. J.; Fiolhais, C. *Phys. Rev. B* **1992**, *46*, 6671–6687.
(18) Becke, A. D. *J. Chem. Phys.* **1993**, *98*, 5648–5652.
(19) Knowles, P. J.; Hampel, C.; Werner, H. J. *J. Chem. Phys.* **1993**, *99*, 5219–5227.
(20) Purvis, G. D.; Bartlett, R. J. *J. Chem. Phys.* **1982**, *76*, 1910–1918.
(21) Møller, C.; Plesset, M. S. *Phys. Rev.* **1934**, *46*, 618–622.
(22) Frisch, M. J.; Trucks, G. W.; Schlegel, H. B.; Scuseria, G. E.; Robb, M. A.; Cheeseman, J. R.; Montgomery, J. A., Jr.; Vreven, T.; Kudin, K. N.; Burant, J. C.; Millam, J. M.; Iyengar, S. S.; Tomasi, J.; Barone, V.; Mennucci, B.; Cossi, M.; Scalmani, G.; Rega, N.; Petersson, G. A.; Nakatsuji, H.; Hada, M.; Ehara, M.; Toyota, K.; Fukuda, R.; Hasegawa, J.; Ishida, M.; Nakajima, T.; Honda, Y.; Kitao, O.; Nakai, H.; Klene, M.; Li, X.; Knox, J. E.; Hratchian, H. P.; Cross, J. B.; Bakken, V.; Adamo, C.; Jaramillo, J.; Gomperts, R.; Stratmann, R. E.; Yazyev, O.; Austin, A. J.; Cammi, R.; Pomelli, C.; Ochterski, J. W.; Ayala, P. Y.; Morokuma, K.; Voth, G. A.; Salvador, P.; Dannenberg, J. J.; Zakrzewski, V. G.; Dapprich, S.; Daniels, A. D.; Strain, M. C.; Farkas, O.; Malick, D. K.; Rabuck, A. D.; Raghavachari, K.; Foresman, J. B.; Ortiz, J. V.; Cui, Q.; Baboul, A. G.; Clifford, S.; Cioslowski, J.; Stefanov, B. B.; Liu, G.; Liashenko, A.; Piskorz, P.; Komaromi, I.; Martin, R. L.; Fox, D. J.; Keith, T.; Al-Laham, M. A.; Peng, C. Y.; Nanayakkara, A.; Challacombe, M.; Gill, P. M. W.; Johnson, B.; Chen, W.; Wong, M. W.; Gonzalez, C.; Pople, J. A. *Gaussian 03*; Gaussian, Inc.: Pittsburgh, PA, **2003**.
(23) Werner, H.-J.; Knowles, P. J.; Lindh, R.; Manby, F. R.; Schütz, M.; Celani, P.; Korona, T.; Rauhut, G.; Amos, R. D.; Bernhardsson, A.; Berning, A.; Cooper, D. L.; Deegan, M. J. O.; Dobbyn, A. J.; Eckert, F.; Hampel, C.; Hetzer, G.; Lloyd, A. W.; McNicholas, S. J.; Meyer, W.; Mura, M. E.; Nicklass, A.; Palmieri, P.; Pitzer, R.; Schumann, U.; Stoll, H.; Stone, A. J.; Tarroni, R.; Thorsteinsson, T. *MOLPRO*, **2006**.
(24) Dolg, M.; Wedig, U.; Stoll, H.; Preuss, H. *J. Chem. Phys.* **1987**, *86*, 866–872.
(25) Peterson, K. A. aug-cc-pwCVTZ-PP basis set for vanadium.
(26) Woon, D. E.; Dunning, T. H. *J. Chem. Phys.* **1993**, *98*, 1358–1371.
(27) Reed, A. E.; Curtiss, L. A.; Weinhold, F. *Chem. Rev.* **1988**, *88*, 899–926.
(28) Wiberg, K. *Tetrahedron* **1968**, *24*, 1083–1096.
(29) Bartell, L. S. *J. Chem. Phys.* **1955**, *23*, 1219.

Table 1. Computed Bond Lengths, Bond Angles, and Relative Energies of the Ground and Low-Lying Excited Electronic States of VCl_2

method	point group	electronic state	ΔE (kJ/mol)	r_e (Å)	α (deg)	imag[a]
CASPT2	$D_{\infty h}$	$^4\Sigma_g^+$	0.0	2.177	180.0	
	$D_{\infty h}$	$^4\Pi_g$	13.9	2.217	180.0	
	$D_{\infty h}$	$^4\Phi_g$	16.1	2.214	180.0	
	$D_{\infty h}$	$^4\Delta_g$	84.1	2.264	180.0	
B3PW91	$D_{\infty h}$	$^4\Sigma_g^+$	0.0	2.195	180.0	0
	C_{2v}[b]	$^4B_2$	25.0	2.234	167.9	0
	$D_{\infty h}$	$^4\Pi_g$	25.1	2.235	180.0	0
	$D_{\infty h}$	$^4\Phi_g$	62.2	2.216	180.0	1
	$D_{\infty h}$	$^4\Delta_g$	68.7	2.277	180.0	0
CCSD(T)	$D_{\infty h}$	$^4\Sigma_g^+$	0.0	2.192	180.0	0
	$D_{\infty h}$	$^4\Pi_g$	33.4	2.237	180.0	0
	$D_{\infty h}$	$^4\Delta_g$	75.5	2.280	180.0	0
	$D_{\infty h}$	$^4\Phi_g$	91.5	2.223	180.0	1
MP2	$D_{\infty h}$	$^4\Sigma_g^+$	0.0	2.181	180.0	0
	$D_{\infty h}$	$^4\Pi_g$	29.7	2.231	180.0	0
	$D_{\infty h}$	$^4\Phi_g$	60.3	2.205	180.0	1
	$D_{\infty h}$	$^4\Delta_g$	68.5	2.273	180.0	0
DFT[c]	$D_{\infty h}$	$^4\Sigma_g^+$		2.181	180.0	
MRCI[d]	$D_{\infty h}$	$^4\Sigma_g^+$		2.251	180.0	

[a] Number of imaginary frequencies. [b] Artificial, see text. [c] Ref 6. [d] Ref 37.

Table 2. Computed Bond Lengths, Bond Angles, and Relative Energies of Low-Lying Electronic States of VCl_3

method	point group	electronic state	ΔE (kJ/mol)	$r_{e,ax}$ (Å)	$r_{e,eq}$ (Å)	α_{eq-eq} (deg)
CASPT2	C_{2v}	$^3A_2$	0.0	2.141	2.157	118.9
	C_{2v}	$^3B_1$	1.2	2.157	2.150	125.9
	D_{3h}	$^3E''$	2.3	2.153		120.0
	D_{3h}	$^3A_2'$	6.4	2.168		120.0
B3PW91	C_{2v}	$^3A_2$	0.0	2.152	2.162	114.1
	C_{2v}	$^3B_1$	0.8	2.169	2.153	124.2
	D_{3h}	$^3E''$	1.7	2.159		120.0
	D_{3h}	$^3A_2'$	8.5	2.177		120.0
CCSD(T)[a]	D_{3h}	$^3E''$		2.152		120.0
MP2	C_{2v}	$^3B_1$	0.0	2.138	2.119	128.1
	C_{2v}	$^3A_2$	1.1	2.112	2.133	114.7
	D_{3h}	$^3E''$	2.6	2.124		120.0
	D_{3h}	$^3A_2'$	8.4	2.153		120.0

[a] From a series of single-point calculations for the $^3E''$ electronic state.

asymmetry parameters of the bond lengths in the ED analysis (vide infra), using the formula $a = 6\kappa(l_T^4)^{-1}(3 - 2l_0^4/l_T^4)^{-1}$, where κ is the asymmetry parameter and l_0 is the vibrational amplitude at 0 K.[30,31] As the bond length differences somewhat depended on the levels of computations (see Tables 1 and 2), we checked how much other sets of parameter differences influenced the final results, and this was taken into account in the estimation of total errors of all parameters. The parameters refined were the VCl_3 bond length, the two monomer bond angles, the vapor content, the asymmetry parameters of the bond lengths refined in groups, and the VCl_2 and VCl_3 vibrational amplitudes. Normal coordinate analyses were performed using the program ASYM20[32] for all species. Vibrational amplitudes were calculated from the computed harmonic vibrational frequencies and force fields for the experimental temperature. However, for VCl_2 and VCl_3, these amplitudes were only used as initial parameters in the analysis, and at further stages they were all refined simultaneously; for refinement **A**, separately, and for refinement **C**, in two groups. The vibrational amplitudes

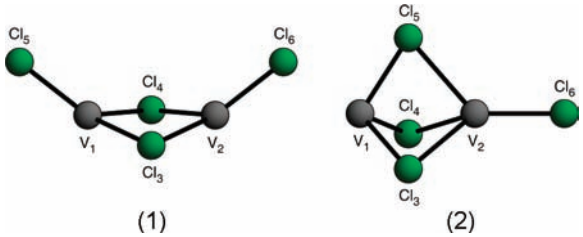

Figure 1. Two different structures of the V_2Cl_4 molecule. 1 refers to the ground-state ($^1A_1$) structure and the D_{2h} ($^1A_{1g}$) and C_{2v} ($^7A_1$) excited state structures, and 2 refers to the excited-state structures of C_s ($^7A''$), C_{3v} (^7E), and C_1 (^1A) symmetry. See Supporting Information for details.

computed for the 1330 K nozzle temperature were somewhat larger than the ones refined during the ED analysis. It turned out that the experimental amplitudes agreed much better with the ones calculated for 1200 K. This lower temperature seems reasonable if we take into account the different dissociation reactions that must have been taking place in the vapor, on the one hand, and the possible cooling on expansion of the gas, on the other.

Results

Computations. The geometrical parameters and relative energies for all computed low-lying electronic states of VCl_2 are given in Table 1. Data from previous studies are also included. All methods agreed that the ground electronic state of VCl_2 is linear with $^4\Sigma_g^+$ symmetry. The next electronic state of $^4\Pi_g$ symmetry is relatively close in energy, within about 14−33 kJ/mol depending on the computational method applied. The energy of the $^4\Delta_g$ state is noticeably higher, while the $^4\Phi_g$ state, also high in energy, is a transition state. The B3PW91 method also produced a Renner−Teller distorted $^4B_2$ state from the $^4\Pi_g$ state, whose energy is almost indistinguishable from the $^4\Pi_g$ state. However, this could be an artifact of broken symmetry, DFT not being able to correctly describe multireference states. Note that for the doubly degenerate $^4\Phi_g$ state our unrestricted Kohn−Sham DFT method gives only one imaginary frequency. For details of different Renner−Teller systems and corresponding force fields see the work of Lee et al.[33]

The computational results for VCl_3 are given in Table 2. Again, different electronic states were taken into consideration. All methods point to a Jahn−Teller distortion of the $^3E''$ structure, leading to a planar C_{2v} symmetry ground-state structure with either $^3A_2$ or $^3B_1$ symmetry. In these lower-symmetry structures, one of the bond angles decreases ("Y-shaped", $^3A_2$) or increases ("T-shaped", $^3B_1$). However, the $^3E''$ undistorted trigonal planar structure is only less than 3 kJ/mol higher in energy than the two Jahn−Teller distorted structures. Furthermore, even the nondegenerate $^3A_2'$ electronic state is only about 6−9 kJ/mol higher in energy than the ground state; thus, all of them can be expected to appear in the vapor phase.

As the V_2Cl_4 molecule was also considered in the earlier study, we computed the structure of this molecule as well for both its high-spin and low-spin states. The geometrical parameters and relative energies of several dimer structures are given in Table S2 in the Supporting Information. Two distinctly different structure types were

(30) Kuchitsu, K. *Bull. Chem. Soc. Jpn.* **1967**, *40*, 505.
(31) Hargittai, M.; Subbotina, N. Y.; Kolonits, M. *J. Chem. Phys.* **1991**, *94*, 7278–7286.
(32) Hedberg, L.; Mills, I. M. *J. Mol. Spectrosc.* **1993**, *160*, 117–142.
(33) Lee, T. J.; Fox, D. J.; Schaefer, H. F., III; Pitzer, R. M. *J. Chem. Phys.* **1984**, *81*, 356–361.

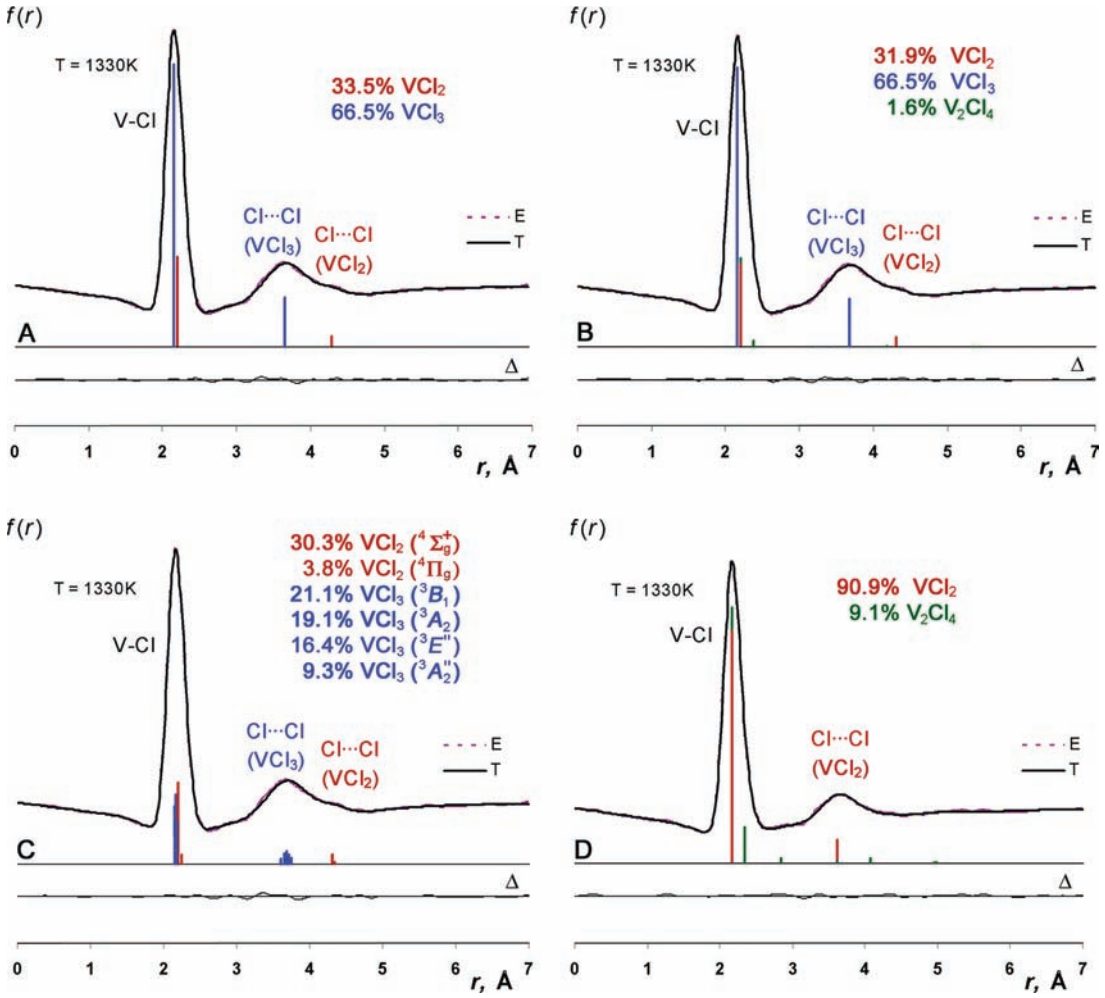

Figure 2. Experimental (E) and calculated (T) electron diffraction radial distributions (**A** through **D**, see text for details) and their differences. **A**, **B**, and **C** are acceptable descriptions of the system; **D** refers to an unacceptable model.

found, as shown in Figure 1; one with two, the other with three halogen bridges with different symmetries (D_{2h}, C_{2v}, C_{3v}, C_s, C_1). The ground-state molecule has an antiferromagnetically coupled low-spin $^1A_1$ electronic state of C_{2v} symmetry with a puckered central four-member ring (see Figure 1). This is in contrast to Cr_2Cl_4, whose minimum-energy structure has C_{2h} symmetry with a planar central ring.[11] Interestingly, while for $CrCl_2$ the high-spin and low-spin dimeric molecules had about the same energy,[11] for VCl_2 the high-spin states are more than 40 kJ/mol higher in energy than the low-spin ground-state structure. On the other hand, in the dimers of iron halides,[34] for example, antiferromagnetic coupling is negligible due to the high energy of these structures.

Electron Diffraction. All three refinement schemes (vide supra) gave equally good agreement with the experiment as illustrated by the molecular intensities (Figure S1, Supporting Information) and radial distributions, Figure 2A−C. Taking into account the high experimental temperature and the large-amplitude bending vibrations of VCl_2, the computed thermal average bond angle is 156.6° ($^4\Sigma_g^+$ state), resulting in a Cl···Cl nonbonded distance of about 4.2 Å. However, the only significant peak on the radial distribution corresponding to nonbonded distances is around 3.8 Å, and that cannot correspond to this species—in fact, this *could* correspond to a highly bent monomeric VCl_2 molecule as shown in Figure 2D (the molecular intensities are shown in Figure S2, Supporting Information), corresponding to the previous publication. However, as seen in Figure 2A, this peak could also correspond to the Cl···Cl distances of VCl_3. In this model, the Cl···Cl contribution of VCl_2 to the radial distribution appears at the shoulder of this peak at about 4.2 Å. Note that for three V−Cl distances there are three Cl···Cl distances in the trichloride, while there is only one Cl···Cl distance for the two V−Cl distances in the dichloride. This is one of the reasons why the latter contribution is so much smaller, besides VCl_2 having a smaller concentration in the vapor (Figure 2A). As VCl_2 might evaporate partly as dimeric molecules, their possible presence was also looked into, but it could only fit in with a very small, at most 1−2%, contribution (Figure 2B). The third variant of the vapor composition that we checked took into consideration that there are several close-lying excited electronic state molecules differing only by small amounts of energy from the ground state and thus can also be expected to be present. As seen in Figure 2C, this version gives a very good agreement with the experiment as well.

(34) Varga, Z.; Kolonits, M.; Hargittai, M. *Inorg. Chem.* **2010**, *49*, 1039–1045.

Table 3. Results of the Electron Diffraction Analyses[a]

	A[b]	B[b]	C[b,c]
		VCl_2	
r_g(V−Cl)	2.213(21)	2.211(19)	2.211(21)
r_e^M(V−Cl)[d]	2.185(23)	2.187(21)	2.183(24)
l(V−Cl)	0.087(2)	0.086(2)	0.087(2)
κ(V−Cl) × 10^{-5}	6.7(3)	5.7(4)	6.8(3)
$\angle_a$(Cl−V−Cl)[e]	155(8)	155(6)	156(8)
amount, %	34(8)	32(7)	30(8)/34(8)[f]
		VCl_3	
r_g(V−Cl)	2.175(8)	2.173(7)	2.173(8)
r_e^M(V−Cl)[d]	2.149(9)	2.149(8)	2.147(10)
l(V−Cl)	0.082(2)	0.81(2)	0.082(2)
κ(V−Cl) × 10^{-5}	5.4(3)	5.0(4)	5.5(3)
$\angle_a$(Cl−V−Cl)[g]	116.1(7)	115.9(5)	116.1(1)
amount, %	66(8)	66(7)	21(8)/66(8)[f]
		V_2Cl_4	
$r_g(V-Cl)_t$[h]		2.211(19)	
$r_g(V-Cl)_b$[h]		2.398(21)	
amount, %		2(1)	
R, %[i]	4.0	3.9	4.0

[a] Thermal average bond lengths (r_g) and estimated equilibrium bond lengths (r_e^M) in Å, angles in degrees, amplitudes (l) in Å, and bond asymmetry parameters (κ) in Å^3. Total errors, including least-squares errors, systematic errors, and errors due to correlation among parameters are given in parentheses. [b] Refinements **A** to **C** correspond to different vapor compositions, see Figure 2A−C and the text for details. [c] The parameters correspond to the $^4\Sigma_g^+$ and $^3E''$ state molecules for VCl_2 and VCl_3, respectively. [d] Experimental equilibrium bond length estimated by Morse-type anharmonic corrections, see text. [e] Thermal average bond angle. Compare with the 156.6° computed thermal-average bond angle for the $^4\Sigma_g^+$ structure (see text). This angle corresponds to a linear equilibrium structure. [f] The first value corresponds to the percentage of the $^4\Sigma_g^+$ and $^3E''$ state molecules, respectively, whose geometries are given in the column. The second number corresponds to the total amount of VCl_2 and VCl_3 molecules in the vapor, respectively; see Figure 2C. [g] Thermal average bond angle, corresponding to a trigonal planar structure (120°) that is the average of the different electronic-state molecules, all of which are possibly present in the vapor (see text). [h] $r_g(V-Cl)_t$, terminal; $r_g(V-Cl)_b$, bridging bond, see also Figure 1. [i] Goodness of fit.

Table 3 presents the results of the electron diffraction analyses. All three vapor compositions give equally good agreement with the experiment; thus, it is not possible to distinguish between them. Fortunately, the bond lengths of neither the VCl_2 nor the VCl_3 monomers are influenced by this uncertainty; therefore, they are well determined.

Discussion

Vanadium dichloride is a linear molecule in its ground electronic state according to all computations. The results of our reanalysis of the earlier electron diffraction data are also consistent with a *linear equilibrium* configuration. The *bent average* structure with a 155(8)° bond angle indicates the consequences of low-frequency−large-amplitude bending vibrations that are especially expressed under the high-temperature (1330 K) experimental conditions. This is in full agreement with the results of computations yielding a 156.6° thermal-average bond angle for the linear $^4\Sigma_g^+$ ground-state VCl_2 molecule. The thermal average bond length (r_g) of VCl_2 is 2.213(21) Å, and the estimated experimental equilibrium bond length (r_e^M) is 2.185(23) Å; the latter, with its very large experimental error, is within the range of the computed values.

Although solid vanadium dichloride was evaporated in the ED experiment, part of it decomposed at the high temperature, producing vanadium trichloride that turned out to be the major component of the vapor with about 66% participation. Computations of VCl_3 led to several electronic states very close in energy, among which a Jahn−Teller-distorted C_{2v}-symmetry planar structure appears to be the ground state. However, as other electronic states are so close in energy, we can expect a complicated topology for them; challenging for future quantum chemical studies. Thus, the high symmetry D_{3h} ($^3E''$) structure appears to be a minimum at the B3PW91 level of theory, which implicates either a dip in the Jahn−Teller Mexican-hat top or that the unrestricted Kohn−Sham treatment is insufficient and multireference methods need to be used to describe the ground and excited electronic states of VCl_3 correctly. Obviously, with such small energy differences (see Table 2), the Jahn−Teller effect is only dynamic, and its detection by experiment can hardly be expected.

Both ground state and excited state molecules are expected to be present in the high-temperature vapor of the ED experiment due to the very small energy differences between the different electronic-state structures, and only their average can be observed. Apart from the 9% trigonal planar $^3A_2''$ excited state (the highest-energy structure among the ones taken into consideration), the other three states (two Jahn−Teller distorted and one undistorted) contribute almost equally (see Table 3 and Figure 2C). Unfortunately, the computed 6° Jahn−Teller distortion of the bond angle from the 120° of the undistorted $^3E''$-symmetry structure does not split the nonbonded Cl···Cl distances sufficiently; therefore, they remain too closely spaced to be distinguished by ED (see Figure 2C).

In contrast, the ED study of another transition metal trihalide, MnF_3, indicated a large Jahn−Teller distortion (about 14° for the bond angle). This resulted in a split of the peak corresponding to the F···F distances on the radial distribution of internuclear distances. This provided unambiguous evidence for the Jahn−Teller effect at similarly high-temperature experimental conditions to those of the VCl_3 study.[35] In MnF_3, the energy difference between the actual ground-state and the undistorted trigonal planar structure was more than 10 times larger than in VCl_3. Gold trifluoride is another example, again, clearly showing the Jahn−Teller effect in the ED experiment.[36]

The thermal average bond length of the VCl_3 molecule is 2.175(8) Å, and its estimated equilibrium bond length from ED is 2.149(9) Å. This is in excellent agreement with the computed equilibrium bond length of the $^3E''$ electronic-state molecule, 2.152 Å [CCSD(T)], that can be considered as the average of the low-electronic-state molecules present in the vapor.

Results of the NBO analyses are given in Table 4. The most noteworthy observation is that the 3d orbital occupations in both the dichloride and the trichloride are larger than expected. Assuming ionic bonding in VCl_2 would require 3

(35) Hargittai, M.; Reffy, B.; Kolonits, M.; Marsden, C. J.; Heully, J. L. *J. Am. Chem. Soc.* **1997**, *119*, 9042–9048.
(36) Reffy, B.; Kolonits, M.; Schulz, A.; Klapotke, T. M.; Hargittai, M. *J. Am. Chem. Soc.* **2000**, *122*, 3127–3134.
(37) Vogel, M.; Wenzel, W. *J. Chem. Phys.* **2005**, *123*, 5.

Table 4. Charges of Vanadium (NBO), Wiberg Bond Indices, and the Natural Electron Configurations (NEC) of Selected VCl_2, V_2Cl_4, and VCl_3 Molecules at B3PW91 Level of Theory

			charges	Wiberg bond indices			NEC
molecule	PG	state	V (e)	V−V	V−$Cl_{ax,t}$	V−$Cl_{eq,b}$	V
VCl_2	$D_{\infty h}$	$^4\Sigma_g^+$	1.04		0.77		4s(0.39)3d(3.47)4p(0.03)4d(0.03)
	C_{2v}	$^4\Pi_g$	1.23		0.61		4s(0.26)3d(3.43)4p(0.04)4d(0.02)
V_2Cl_4	C_{2v}	$^1A_1$	0.98	0.07	0.80	0.43	4s(0.32)3d(3.62)4p(0.02)4d(0.05)
	C_{2v}	$^7A_1$	0.85	0.40	0.79	0.47	4s(0.33)3d(3.69)4p(0.05)4d(0.07)4f(0.01)
VCl_3	C_{2v}	$^3A_2$	0.86		1.09	1.00	4s(0.34)3d(3.54)4p(0.04)4d(0.08)4f(0.01)
	C_{2v}	$^3B_1$	0.86		0.95	1.07	4s(0.34)3d(3.54)4p(0.04)4d(0.08)4f(0.01)
	D_{3h}	$^3A_2'$	1.18		0.88		4s(0.25)3d(3.43)4p(0.04)4d(0.09)4f(0.01)

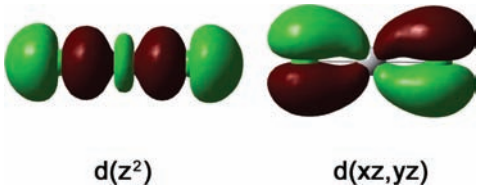

Figure 3. Selected bonding MOs for VCl_2 ($^4\Sigma_g^+$), indicating the participating 3d orbital of vanadium.

electrons in the 3d orbitals, while the NEC (natural electron configuration) gives 3.5e for that orbital. This increase indicates back-donation of electrons from the chlorine p orbitals and supposes a certain covalent character for the bonds that is also shown by the Wiberg index, 0.77, for the ground-state VCl_2 molecule. Figure 3 shows the relevant MOs for VCl_2. The charge of +1.0 on the vanadium atom is consistent with the above comments.

The results of the NBO analysis of VCl_3 are even more surprising. Instead of the expected 2 electrons in the 3d orbitals of vanadium, there is the same amount of electrons (3.5e) in these orbitals as in VCl_2. The covalent character of the V−Cl bond is stronger (Wiberg indices are about 1.0 for the ground state VCl_3 molecule), and the vanadium charge is about the same as in the dichloride. The corresponding molecular orbitals are shown in Figure 4, nicely demonstrating the covalent bonding and the vanadium d character involved.

The terminal V−Cl bonds in the vanadium dichloride dimer are even more covalent than the bonds in the monomer, with the bridging bonds having smaller covalent character. The low-spin and high-spin structures of C_{2v} symmetry differ mainly in that in the latter there is a noticeable V···V interaction (Wiberg index 0.4).

In summary, vanadium halides appear to be difficult objects for both computations and experiments. This study indicates that electron diffraction alone is not capable of giving an unambiguous solution to their structures. As Figure 2A−D indicate, not only different vapor contents

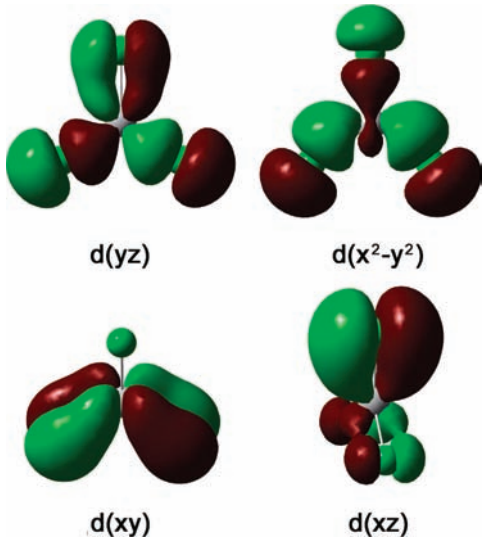

Figure 4. Selected bonding MOs for VCl_3 ($^3A_2$), indicating the corresponding 3d orbital of vanadium.

but also very different molecular shapes of the same molecule can give acceptable agreements between the experimental and calculated distributions (Figure 2A−C correspond to a linear while Figure 2D to strongly bent VCl_2). Hence, the joint application of experimental and computational techniques has proved to be essential and yielded reliable structures.

Acknowledgment. Z.V. and M.H. acknowledge the Hungarian Scientific Research Fund (OTKA K 60365) for support. B.V. thanks the Institute for Advanced Study (IAS) for financial support.

Supporting Information Available: Experimental electron diffraction molecular intensities (Table S1 and Figures S1−S2); computed structures of different electronic states of V_2Cl_4 (Table S2); and vibrational frequencies of VCl_2, VCl_3, and V_2Cl_4 (Tables S3−S5). This material is available free of charge via the Internet at http://pubs.acs.org.